

Superposed nonlinear waves in coherently coupled Bose-Einstein condensates

R. Babu Mareeswaran, T. Kanna*

Post Graduate and Research Department of Physics, Bishop Heber College, Tiruchirapalli-620 017, Tamil Nadu, India

Abstract

We study the dynamics of superposed nonlinear waves in coherently coupled Gross-Pitaevskii (CCGP) equations with constant (autonomous system) and time varying (non-autonomous system) nonlinearity co-efficients. By employing a linear transformation, the autonomous CCGP system is converted into two separate scalar nonlinear Schrödinger equations and we show that linear superposition of different nonlinear wave solutions of these scalar equations results into several kinds of nonlinear coherent structures namely, coexisting rogue wave-Ma breather, Akhmediev-Ma breathers, collision and bound states of Ma breathers and solitons. Next, the non-autonomous CCGP system is converted into an autonomous CCGP system with a similarity transformation. We show an interesting possibility of soliton compression and appearance of creeping solitons for kink-like and periodically modulated nonlinearity coefficient.

Keywords: Coherently coupled Gross-Pitaevskii equation, similarity transformation, solitons, rogue waves, breathers (Ma and Akhmediev)

1. Introduction

Nonlinear wave phenomena are of wide physical and mathematical interest as they arise in diverse areas of science such as nonlinear optics, fluid dynamics, lattice dynamics, plasma physics, bio-physics and Bose-Einstein condensates (BEC) [1, 2, 3, 4]. In the context of BECs several kinds of nonlinear coherent structures, such as, solitons [5], discrete breathers [6], rogue waves [7], Faraday waves [8], gap solitons [9] and vortices [10] have been observed. Particularly, the multicomponent BECs host rich dynamical behaviors because of the vector order parameters. These systems display interesting effects such as Josephson effect [11], Efimov effect [12], spin textures [13], spin-orbit coupling [14], just to cite a few of them. The fundamental multicomponent BEC is the two component BEC. Such two-component BEC has been realized by using a mixture of atoms with two hyperfine states of ^{87}Rb [15]. The theoretical studies on spin dipole oscillations [16], vortex pairs [17], phase transition [18], localized waves [19] and bosons in optical lattices [20] emphasize the need for investigation of BECs with coherent (phase-dependent) coupling.

Observing solitons in multicomponent condensates is one of the current research topics. The formation and dynamical properties of solitons in BECs are determined by the nature of their two-body atomic interactions, i.e., the sign of the s -wave scattering length which may be positive (negative) for repulsive (attractive) interatomic interactions. The s -wave scattering length and hence the nonlinearity co-efficient can be controlled by means of Feshbach resonance [21]. If we use a time-dependent magnetic field, the strength of the nonlinear interaction can be tuned by time-dependent Feshbach resonance. In real experiments, various forms of time-dependence of nonlinearity have been explored [22]. In theoretical studies, many authors have thoroughly studied the dynamics of BECs for several forms of time (or) spatial dependent nonlinearity co-efficients (see, e.g., [23, 24, 25] and references therein). In the present work, we will be interested in a system of two coupled Gross-Pitaevskii equations with a coherent coupling between both components [26, 18] along with time-varying scattering lengths and external potential.

*Corresponding author

Email address: kanna_phy@bhc.edu.in (T. Kanna)

On the other hand, study of nonlinear waves like, protean rogue waves and breathers in BECs is also one of the main objectives of modern day research [4, 7, 27]. A formal mathematical description of single rogue wave is provided by the nonlinear Schrödinger (NLS) equation in the self-focusing regime [28]. Here the mechanism which leads to the generation of rogue waves is nonlinear wave mixing, that generates modulation instability (MI) of the continuous wave (CW) background [29]. The nonlinear development of MI is described by families of exact breathers. A special member of this solution family is the Peregrine soliton [30], which represents a wave that is localized both in space and time dimensions. In recent years, rogue waves and breathers have attracted much attention [31, 32, 27, 33]. A number of recent reviews have attempted to summarize the study of rogue waves in different contexts [34]. The space-periodic breather type solution of NLS system has been obtained by Akhmediev et al., [35] and the time-periodic solution of NLS was derived by Ma [36].

In this paper, we carry out a thorough analysis of the dynamics of superposed nonlinear waves in autonomous and non-autonomous coherently coupled Gross-Pitaevskii (CCGP) system. The autonomous CCGP equations considered in this paper are shown to be integrable in Ref. [37] and Kanna et al., have constructed the explicit soliton solutions of the underlying equation by applying a non-standard Hirota's bilinearization procedure in Ref. [38]. Very recently, in Ref. [39] by applying the Darboux transformation method, the soliton and rogue wave solutions of CCGP equations have been constructed. In the present work, we decouple the autonomous CCGP equations into two uncoupled NLS equations and make use of their different nonlinear wave solutions profitably to construct the superposed nonlinear wave solution of the autonomous CCGP equations and study their subsequent dynamics. Then we make use of these superposed nonlinear waves to obtain the nonlinear wave solutions of the non-autonomous CCGP equations with the aid of a similarity transformation. We have observed an interesting soliton phenomenon namely, soliton compression and also shown the existence of creeping soliton. The obtained solutions are new and display rich dynamical features that can find applications in atom interferometry and matter wave switches.

The remaining part of this paper is arranged as follows: We present the model equation and its physical significance in Sec. II. In Sec. III, the set of autonomous CCGP equations is converted into two independent NLS systems. We review the solutions of scalar (decoupled) NLS system and discuss their properties in Sec. III A. Sec. III B, deals with the interesting coherent structures of superposed nonlinear waves, namely colliding Ma breathers, coexisting rogue wave and Ma breathers, and coexisting Ma and Akhmediev breathers. In Sec. IV, we convert the non-autonomous CCGP system into an integrable autonomous CCGP system by using a similarity transformation. Also we clearly bring out the role of variable nonlinearity by considering two types of time-varying nonlinearities namely, kink-like and periodic modulated (Mathieu function) nonlinearity. Finally, the results are summarized in Sec. V.

2. The Model

Here we consider the quasi-one-dimensional (cigar-shaped) BEC. For this case, the three dimensional CCGP system can be reduced to an one dimensional system and we can write the governing equations in dimensionless form as [26, 18]

$$i \frac{\partial \psi_1}{\partial t} = L_1 \psi_1 - \alpha_1 (|\psi_1|^2 + 2|\psi_2|^2) \psi_1 - \alpha_2 \psi_2^2 \psi_1^*, \quad (1a)$$

$$i \frac{\partial \psi_2}{\partial t} = L_2 \psi_2 - \alpha_1 (2|\psi_1|^2 + |\psi_2|^2) \psi_2 - \alpha_2 \psi_1^2 \psi_2^*, \quad (1b)$$

where $L_i = -\partial_x^2 + U_i(x, t)$ with $i = 1, 2$. Here, we measure the length and energy in units of $a_{ho} = \sqrt{\hbar/m\omega_\perp}$, where a_{ho} is the characteristic length of the condensate and $\hbar\omega_\perp$, in which ω_\perp is the transversal frequency. In Eqs. (1), ψ_j ($j = 1, 2$) are the condensate wave functions; the coefficients α_1 and α_2 introduce incoherent and coherent coupling between the two components and they can be tuned using Feshbach resonance mechanism and $U_i(x, t)$ ($i = 1, 2$) are the external potentials. For the homogeneous system the external potentials $U_i(x, t) = 0$.

The physical significance of the above proposed model can be realized in the following two contexts. (i) In spin-1 BECs, the governing equation is three-component GP equations with the components [i.e., $\Psi = (\psi_{+1}/\sqrt{2}, \psi_0, \psi_{-1})^T$]

corresponding to the three values of the vertical spin projection, $m_F = -1, 0, +1$ (see Eqs. (4) and (5) in ref. [40]). For the special case ($\psi_{+1} = \psi_{-1}$ and $c_0 = c_2 = -c$), the set of three-component GP equations is reduced to two component GP system (1) with $\alpha_1 = \alpha_2 = c$. (ii) In the context of nonlinear optics, the model equation exactly same as that of (1) governs the pico-second pulse propagation in nonlinear Kerr media with low birefringence or beam propagation in weakly anisotropic media and is usually referred as coherently coupled nonlinear Schrödinger equations [41, 38].

Apart from these, Eqs. (1) can also be viewed as the continuum limit of the model for the discrete coupled atomic condensates describing the four-wave mixing effects discussed in ref. [42]

3. Autonomous CCGP system

First, we consider the homogeneous binary condensates ($U_i(x, t) = 0$) with constant nonlinearity co-efficient $\alpha_1 = \alpha_2 = \alpha$ in Eq. (1). Here α is a real integer and is independent of time. The resulting equations can be expressed as

$$i \frac{\partial \psi_1}{\partial t} = -\frac{\partial^2 \psi_1}{\partial x^2} - \alpha(|\psi_1|^2 + 2|\psi_2|^2)\psi_1 - \alpha\psi_2^2\psi_1^*, \quad (2a)$$

$$i \frac{\partial \psi_2}{\partial t} = -\frac{\partial^2 \psi_2}{\partial x^2} - \alpha(2|\psi_1|^2 + |\psi_2|^2)\psi_2 - \alpha\psi_1^2\psi_2^*. \quad (2b)$$

In this paper, we refer to Eqs. (2) as autonomous CCGP equations. These autonomous CCGP equations are integrable [37] and several interesting soliton solutions have been obtained in Ref.[38] by applying a non-standard Hirota's bilinearization technique. We note that Eqs. (2) with $\alpha = 2$, can be decoupled into two independent NLS equations of the form

$$iu_{j,t} + u_{j,xx} + 2u_j^*u_j^2 = 0, \quad j = 1, 2, \quad (3)$$

by applying a linear transformation

$$\psi_1(x, t) = \frac{1}{2}(u_1 + u_2), \quad (4a)$$

$$\psi_2(x, t) = \frac{1}{2}(u_1 - u_2), \quad (4b)$$

where u_1 and u_2 are arbitrary analytic functions of x and t and satisfy the NLS equation (3).

The above NLS system (3) is completely integrable and has been investigated extensively by using various analytical methods. Interestingly, it admits many kinds of nonlinear wave solutions such as solitons, rogue waves and breathers (including Ma and Akhmediev breathers) [43, 44] and they have been experimentally observed under different contexts. Particularly the Peregrine soliton of the NLS system has been recently observed experimentally in nonlinear optics [45].

In this paper, we address the dynamical features of superposition of these various structures which are also possible solutions of Eqs. (2). As a prelude we briefly revisit some of the interesting nonlinear wave solutions of the scalar NLS system (3) in the following sub-section.

3.1. Revisit of nonlinear waves in the NLS system

(i) Bright one-soliton

The bright one-soliton solution u_1 of the NLS equation (3) with $j = 1$ is obtained as [46]

$$u_1(x, t) = k_R^{(1)} \text{sech}(z_2^{(1)})e^{iz_1^{(1)}}, \quad (5)$$

where $z_1^{(1)} = k_I^{(1)}x + ((k_R^{(1)})^2 - (k_I^{(1)})^2)t + \eta_I^{(1)}$, $z_2^{(1)} = k_R^{(1)}(x - 2k_I^{(1)}t) + \eta_R^{(1)} + R^{(1)}$, and $R^{(1)} = \ln\left[\frac{1}{2k_R^{(1)}}\right]$. The above one-soliton solution u_1 is characterized by four real parameters $k_R^{(1)}$, $k_I^{(1)}$, $\eta_R^{(1)}$ and $\eta_I^{(1)}$. Similar solution for u_2 can be obtained by replacing the superscript (1) by (2). Here and in the following R and I appearing in the suffices of the soliton parameters denote the real and imaginary parts, respectively. The amplitude and velocity of the NLS soliton can be controlled by tuning $k_R^{(1)}$ and $k_I^{(1)}$, respectively, while the soliton position depends on the parameter $\eta_R^{(1)}$.

(ii) *Bright two-soliton*

The bright two-soliton solutions of the above two different NLS systems (3) (u_j with $j = 1$ corresponds to the solution of the first NLS system and $j = 2$ corresponds to the solution of the second NLS system) are given by [46]

$$u_j(x, t) = \frac{G^{(j)}}{F^{(j)}}, \quad j = 1, 2, \quad (6a)$$

where

$$G^{(j)} = e^{\eta_1^{(j)}} + e^{\eta_2^{(j)}} + e^{\eta_1^{(j)} + \eta_1^{(j)*} + \eta_2^{(j)} + \delta_1^{(j)}} + e^{\eta_1^{(j)} + \eta_2^{(j)} + \eta_2^{(j)*} + \delta_2^{(j)}}, \quad (6b)$$

$$F^{(j)} = 1 + e^{\eta_1^{(j)} + \eta_1^{(j)*} + R_1^{(j)}} + e^{\eta_1^{(j)} + \eta_2^{(j)*} + \delta_0^{(j)}} + e^{\eta_2^{(j)} + \eta_1^{(j)*} + \delta_0^{(j)*}} + e^{\eta_2^{(j)} + \eta_2^{(j)*} + R_2^{(j)}} + e^{\eta_1^{(j)} + \eta_1^{(j)*} + \eta_2^{(j)} + \eta_2^{(j)*} + R_3^{(j)}}. \quad (6c)$$

In the above solution, $\eta_1^{(j)} = k_1^{(j)}x + i(k_1^{(j)})^2t + \eta_1^{(j)(0)}$, $\eta_2^{(j)} = k_2^{(j)}x + i(k_2^{(j)})^2t + \eta_2^{(j)(0)}$, $e^{R_1^{(j)}} = \frac{1}{(k_1^{(j)} + k_1^{(j)*})^2}$, $e^{R_2^{(j)}} = \frac{1}{(k_2^{(j)} + k_2^{(j)*})^2}$, $e^{\delta_0^{(j)}} = \frac{1}{(k_1^{(j)} + k_2^{(j)})^2}$, $e^{\delta_0^{(j)*}} = \frac{1}{(k_1^{(j)*} + k_2^{(j)*})^2}$, $e^{\delta_1^{(j)}} = \frac{(k_1^{(j)} - k_2^{(j)})^2}{(k_1^{(j)} + k_1^{(j)*})^2(k_1^{(j)*} + k_2^{(j)})^2}$, $e^{\delta_2^{(j)}} = \frac{(k_2^{(j)} - k_1^{(j)})^2}{(k_1^{(j)} + k_2^{(j)})^2(k_2^{(j)*} + k_2^{(j)})^2}$ and $e^{R_3^{(j)}} = \frac{(k_1^{(j)} - k_2^{(j)})^2(k_1^{(j)*} - k_2^{(j)*})^2}{(k_1^{(j)} + k_1^{(j)*})^2(k_1^{(j)*} + k_2^{(j)})^2(k_1^{(j)} + k_2^{(j)*})^2(k_2^{(j)} + k_2^{(j)*})^2}$.

The bright two-soliton solution of the NLS equation is characterized by four complex parameters $k_1^{(j)}$, $k_2^{(j)}$, $\eta_1^{(j)(0)}$ and $\eta_2^{(j)(0)}$. Here the real parts of $k_1^{(j)}$ and $k_2^{(j)}$ control the amplitude of the respective soliton, while their imaginary parts influence the velocity. One can observe two kinds of dynamics from the above two-soliton solution: two-soliton bound state with beating for same soliton velocities ($k_{1I}^{(1)} = k_{2I}^{(1)}$) and a head-on elastic soliton collision for equal but opposite soliton velocities ($k_{1I}^{(1)} = -k_{2I}^{(1)}$).

(iii) *Rogue wave*

Rogue waves are nothing but a sudden peak (hump) localized both in space and time with maximum amplitude on a continuous wave background. The rogue wave (rational) solutions (u_j , $j = 1, 2$) of the two independent NLS systems (3) obtained in Ref. [47] can be written as

$$u_j(x, t) = \left[1 - \frac{2(1 + 4i|\delta^{(j)}|^2t)}{2|\delta^{(j)}|^2(x^2 + 4|\delta^{(j)}|^2t^2 + \frac{1}{4|\delta^{(j)}|^2})} \right] \times \delta^{(j)} e^{2i|\delta^{(j)}|^2t}, \quad j = 1, 2. \quad (7)$$

Here the arbitrary complex parameter $\delta^{(j)}$ influences the amplitude as well as the width of the rogue wave in the j^{th} NLS system. In general, the amplitude of rogue wave is three-times (or more) higher than the background carrier wave.

(iv) *Akhmediev breather*

Akhmediev breather (AB) solution (u_j , where $j = 1$ corresponds to the solution of the first NLS system and $j = 2$ corresponds to the solution of the second NLS system) of the two independent NLS equations (3) is given by

$$u_j(x, t) = \left[\frac{\cosh(\Omega t - 2ia^{(j)}) - \cos(a^{(j)}) \cos(b^{(j)}x)}{\cosh(\Omega t) - \cos(a^{(j)}) \cos(b^{(j)}x)} \right] \times e^{2it}, \quad j = 1, 2, \quad (8)$$

where $\Omega = 2 \sin(2a^{(j)})$, $b^{(j)} = 2 \sin(a^{(j)})$ and $a^{(j)} \in \mathbb{R}$. The role of parameter $a^{(j)}$ in AB is directly related to the number of breathers and inversely related to its maximum amplitude. To be more precise, for increasing value of $a^{(j)}$ the number of breathers over a definite region increases but their amplitude decreases, whereas the reverse scenario takes place for decreasing value of $a^{(j)}$ [43].

(v) *Ma breather*

The Ma breather (MB) solutions of the two independent NLS equations (3) can be expressed as

$$u_j(x, t) = \left[\frac{\cos(\Omega t - 2ia^{(j)}) - \cosh(a^{(j)}) \cosh(b^{(j)}x)}{\cos(\Omega t) - \cosh(a^{(j)}) \cosh(b^{(j)}x)} \right] \times e^{2it}, \quad j = 1, 2, \quad (9)$$

where $\Omega = 2 \sinh(2a^{(j)})$, $b^{(j)} = 2 \sinh(a^{(j)})$ and $a^{(j)} \in \mathbb{R}$. These Ma breathers are localized in spatial (x) coordinate and periodic in time (t) coordinate. The effect of parameter $a^{(j)}$ is straightforward in the case of MB, where the number of breathers as well as their maximum amplitude increases (decreases) when $a^{(j)}$ is increased (decreased) [43].

3.2. Dynamics of superposed nonlinear waves

In the starting of this section, we have shown that the solution of the autonomous CCGP system (2) can be obtained by superposing the solutions of two different NLS systems. Following that, we revisit several nonlinear wave solutions of NLS system.

Now we look into the various combinations of these solutions discussed in Sec. IIA and construct several superposed solutions of the autonomous CCGP system. This will give rise to the possibility of non-trivial localized nonlinear coherent structures in the autonomous CCGP system.

Case (i) Superposition of two different one-soliton solutions

To start with, we consider two different one-soliton solution forms obtained from (5) with $j = 1$ and 2 and write down the solutions ψ_j , ($j = 1, 2$) of the autonomous CCGP system using (4).

First we superimpose two one-solitons travelling with different amplitudes and opposite velocities. The resultant structure is a head on collision of two soliton in the ψ_1 and ψ_2 components. This is depicted in Fig. 1.

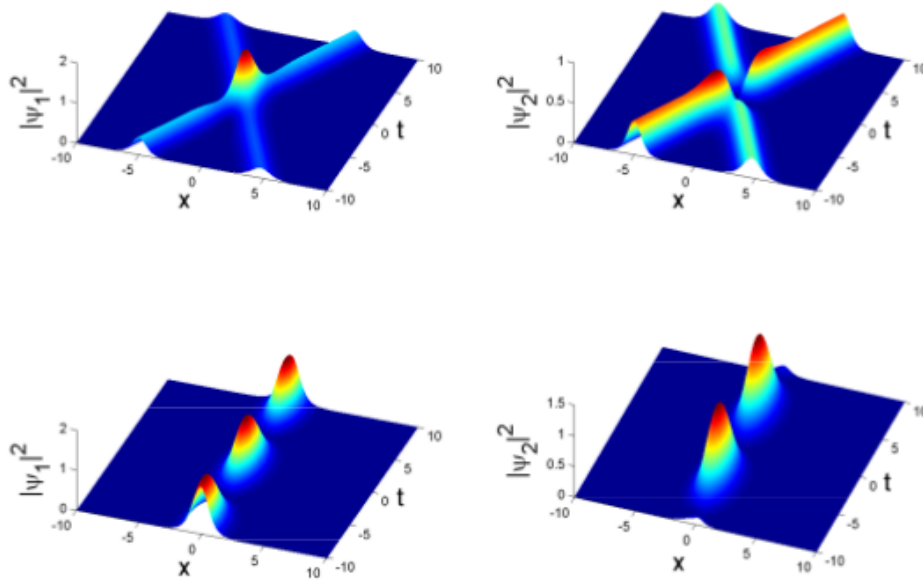


Figure 1: Superposition of two different one-soliton. Top panel: Soliton collision with parameters $k_R^{(1)} = 1.3$, $k_I^{(1)} = 0.25$, $k_R^{(2)} = 1$, $k_I^{(2)} = -0.25$, $\eta_R^{(1)(0)} = \eta_R^{(2)(0)} = 1$ and $\eta_I^{(1)(0)} = \eta_I^{(2)(0)} = 0.2$; Bottom panel: Bound soliton for the parametric choice $k_R^{(1)} = 1.3$, $k_I^{(1)} = 0$, $k_R^{(2)} = 1$, $\eta_R^{(1)(0)} = \eta_R^{(2)(0)} = 1$ and $\eta_I^{(1)(0)} = \eta_I^{(2)(0)} = 0.2$.

The expression for $|\psi_1|^2 = \frac{1}{4} [(k_R^{(1)})^2 \text{sech}^2(z_2^{(1)}) + (k_R^{(2)})^2 \text{sech}^2(z_2^{(2)}) + 2k_R^{(1)}k_R^{(2)} \text{sech}(z_2^{(1)})\text{sech}(z_2^{(2)}) \cos(z_1^{(1)} - z_1^{(2)})]$ and $|\psi_2|^2 = \frac{1}{4} [(k_R^{(1)})^2 \text{sech}^2(z_2^{(1)}) + (k_R^{(2)})^2 \text{sech}^2(z_2^{(2)}) - 2k_R^{(1)}k_R^{(2)} \text{sech}(z_2^{(1)})\text{sech}(z_2^{(2)}) \cos(z_1^{(1)} - z_1^{(2)})]$. At the origin $[(x, t)=0]$, the intensity of the resulting superposed coherent structure attains a maximum value in the ψ_1 component while it reaches a minimum value in the ψ_2 component. This is a consequence of conservation of total energy ($\int (|\psi_1|^2 + |\psi_2|^2) dt = \text{const.}$). If we choose $k_I^{(1)}$ and $k_I^{(2)}$ to be zero or to be equal with $z_1^{(1)} \neq z_1^{(2)}$, we obtain soliton bound state with oscillations along t axis. This is clearly shown in the bottom panel of Fig. 1. Another interesting possibility arises for $k^{(1)}=k^{(2)}$, where the superposed soliton exists only in the ψ_1 component and is absent in the ψ_2 component. Thus we can engineer the nature of soliton propagation by tuning the $k^{(j)}$ parameters appropriately.

Case (ii) Superposition of one-soliton (u_1) with two-soliton (u_2)

Next we construct ψ_1 and ψ_2 (see Eq. (4)) by superposing one-soliton solution (u_1) with two-soliton solution (u_2). Fig. 2 depicts the density plot of such superposed nonlinear coherent structures. Here we discuss two possible

interesting coherent structures in the ψ_1 and ψ_2 components: (i) superposition of bound soliton (which can be obtained by setting same values for the imaginary parts of $k_1^{(2)}$ and $k_2^{(2)}$ parameters in the two-soliton solution) with one soliton. This is shown in the top panel of Fig. 2. There is another possibility which is shown in the middle panel of figure (2). Here the coherent structure displays a collision of bound soliton with a single soliton. Specifically a double-hump breather is converted into a single-hump breather with increased intensity after collision. (ii) superposition of two-soliton with one-soliton in which all the three solitons are travelling at different velocities. To obtain this we set different values for $k^{(1)}$, $k_1^{(2)}$ and $k_2^{(2)}$ (see bottom panel of Fig. 2). The resulting coherent structure is an interaction of three independent solitons.

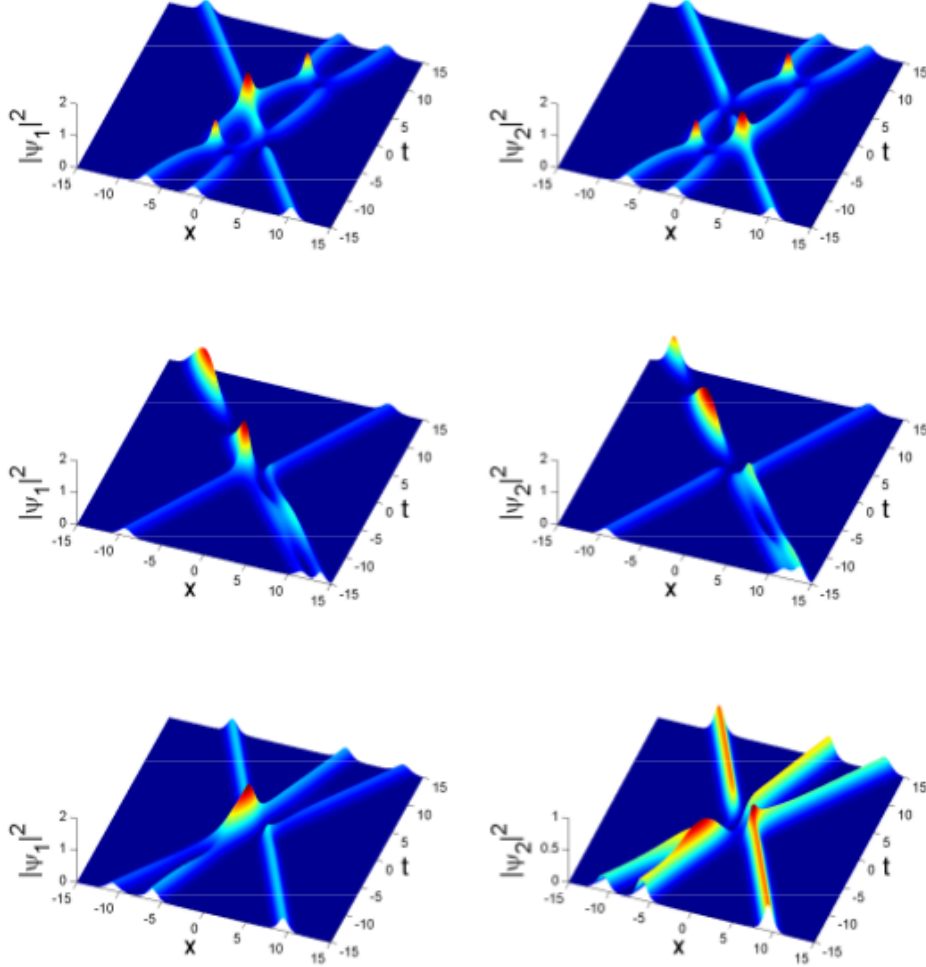


Figure 2: Superposition of single- and two- solitons. Top Panel: Collision of bound state and soliton with parameters $k^{(1)} = 1.2 - 0.35i$, $k_1^{(2)} = 1.2 + 0.2i$, $k_2^{(2)} = 1 + 0.2i$, $\eta_1^{(2)(0)} = 1$, $\eta_2^{(2)(0)} = 1$, $\eta_R^{(1)} = 1$, and $\eta_I^{(1)} = 0.2$; Middle Panel: Collision of one- soliton with bound soliton with parameters $k^{(1)} = 1 - 0.4i$, $k_1^{(2)} = 1.25 - 0.4i$, $k_2^{(2)} = 1 + 0.3i$, $\eta_1^{(2)(0)} = 1$, $\eta_2^{(2)(0)} = 1$, $\eta_R^{(1)} = 1$, and $\eta_I^{(1)} = 0.1$; Bottom Panel: Three soliton collision with parameters $k^{(1)} = 1.2 + 0.2i$, $k_1^{(2)} = 1.3 - 0.25i$, $k_2^{(2)} = 1 + 0.35i$ and all other parameters are same as given in the top panel.

Case (iii) Superposition of one-soliton (u_1) with Akhmediev breather (u_2)

In this case, we choose the one-soliton solution for u_1 as given by Eq. (5) and Akhmediev breather (spatially periodic) form for u_2 in (4). After superposing a stationary soliton ($k_I^{(1)} = 0$) with Akhmediev breather, we obtain special nonlinear coherent structures in which the Ma and Akhmediev breathers coexist in both ψ_1 and ψ_2 components. Such coherent structures are shown in Fig. 3. For solitons with non-zero velocity, also similar co-existence of Ma and Akhmediev breathers exists.

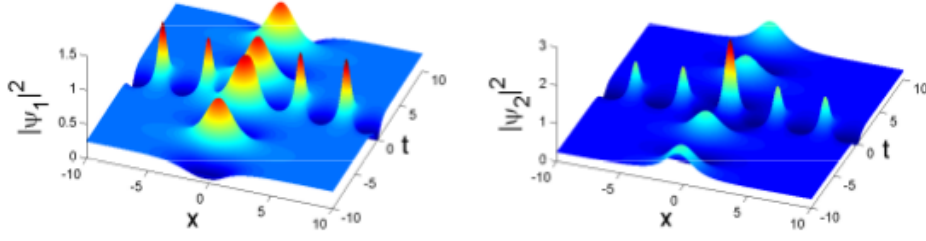


Figure 3: Superposition of one-soliton with Akhmediev breather. The parameters $k_R^{(1)} = 0.9$, $k_I^{(1)} = 0$, $a^{(2)} = 1$, $\eta_R^{(1)} = 1$, and $\eta_I^{(1)} = 0.2$.

Case (iv) Superposition of one-soliton (u_1) with Ma breather (u_2)

In this case, we choose the one-soliton solution as given by Eq. (5) and MB (time periodic) form for u_2 in Eq. (4). In ψ_1 and ψ_2 components, we get nonlinear coherent structures akin to the collision of two MBs. This is shown in Fig. 4 for illustrative purpose. If we choose the soliton velocity to be zero, the two MBs overlap with each other.

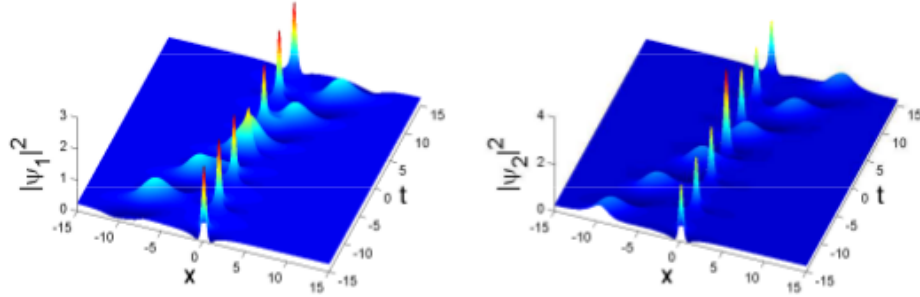


Figure 4: Superposition of one-soliton with Ma breather. The parameters are $k_R^{(1)} = 0.9$, $k_I^{(1)} = 0.3$, $a^{(2)} = 0.2$, $\eta_R^{(1)} = -1$, and $\eta_I^{(1)} = 0.2$.

Case (v) Superposition of one-soliton (u_1) with a Rogue wave (u_2)

In this case, for u_1 and u_2 in (4), we choose one soliton and rogue wave solution, respectively. When we superpose these two types of nonlinear waves using the transformation (4), the resultant structure is the coexistence of MB and rogue wave in the ψ_1 and ψ_2 components. This is depicted in figure 5.

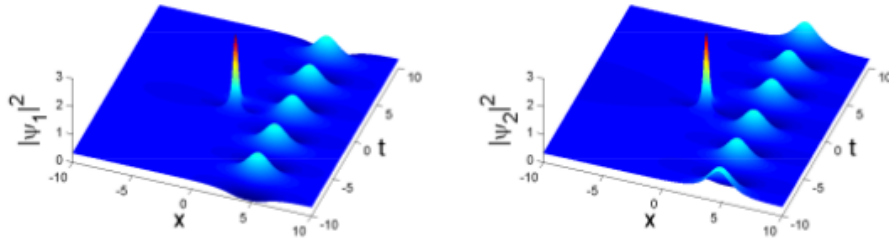


Figure 5: Superposition of one-soliton with rogue wave with parameters $k_R^{(1)} = 1$, $k_I^{(1)} = 0$, $\eta_R^{(1)} = -4$, $\eta_I^{(1)} = 0.2$ and $\delta^{(2)} = \sqrt{1.3}$.

Here we note that the soliton is converted into a MB. This can be understood by writing down the detailed expression for $|\psi_1|^2$ and $|\psi_2|^2$. We find $|\psi_1|^2 = \frac{1}{4} (|\lambda|^2 + (k_R^{(1)})^2 \text{sech}^2(z_2^{(1)}) + k_R^{(1)} \text{sech}(z_2^{(1)}) [2\lambda_R \cos(\chi) - 2\lambda_I \sin(\chi)])$ and

$|\psi_2|^2 = \frac{1}{4} \left(|\lambda|^2 + (k_R^{(1)})^2 \text{sech}^2(z_2^{(1)}) + k_R^{(1)} \text{sech}(z_2^{(1)}) [-2\lambda_R \cos(\chi) + 2\lambda_I \sin(\chi)] \right)$, where $\chi = 2|\delta^{(2)}|^2 t - z_1^{(1)}$ and $\lambda = \delta^{(2)} \left[1 - \frac{2(1+4i|\delta^{(2)}|^2 t)}{2|\delta^{(2)}|^2(x^2+4|\delta^{(2)}|^2 t^2 + \frac{1}{4|\delta^{(2)}|^2})} \right]$. We observe that the interference terms for $|\psi_1|^2$ and $|\psi_2|^2$ involve *cosine* and *sine* functions. Ultimately, this results in breathing oscillations in the soliton intensity along the t axis thereby converting it into a MB.

Case (vi) Superposition of two-soliton solution (u_1) with Rogue wave (u_2)

Here we choose two-soliton solution and rogue wave for u_1 and u_2 , respectively, in Eq. (4). The two colliding solitons are now converted into interacting MBs. As a result of this we get a nonlinear coherent structure comprising of a rogue wave and two colliding MBs. This is shown in the top panel of Fig. 6 for the choice of parameters $k_1^{(1)} = 1 + 0.2i$, $k_2^{(1)} = 1 - 0.2i$ and $\delta^{(2)} = \sqrt{1.5}$. If we choose the imaginary part of $k_1^{(1)}$ and $k_2^{(1)}$ parameters to be zero, which means the velocities of respective solitons are zero, then we obtain bound state with breathing oscillations (see bottom panel).

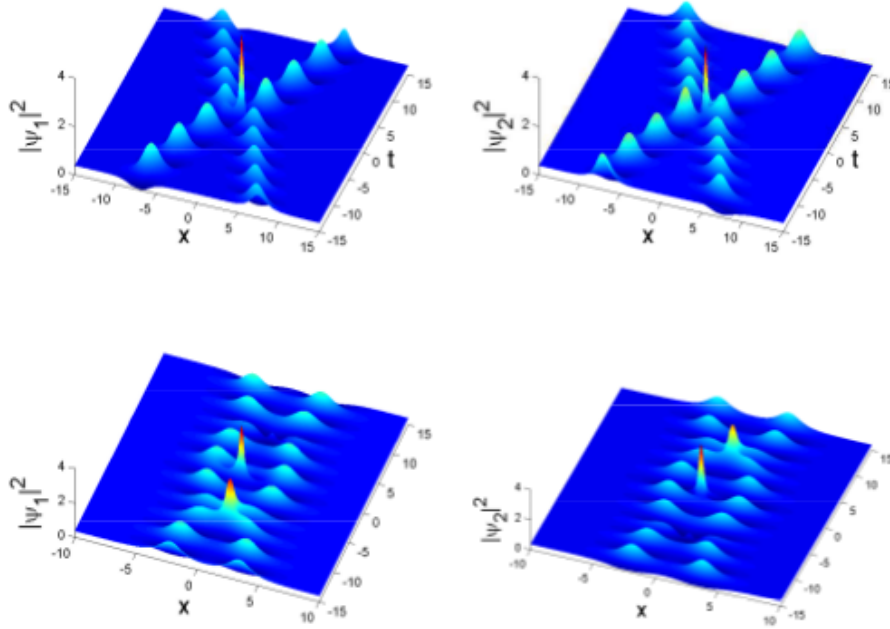


Figure 6: Superposition of two-soliton with rogue wave. Top Panel: Coexistence of interactions between two breathers and rogue wave with parameters are $k_1^{(1)} = 1.25 + 0.2i$, $k_2^{(1)} = 1 - 0.2i$, $\delta^{(2)} = \sqrt{1.5}$, and $\eta_1^{(1)(0)} = \eta_2^{(1)(0)} = 2.5 + i$. Bottom panel: Breather bound states with parameters $k_1^{(1)} = 1.2$, $k_2^{(1)} = 1$, $\delta^{(2)} = \sqrt{1.5}$ and $\eta_1^{(1)(0)} = \eta_2^{(1)(0)} = 2.5 + i$.

Case (vii) Superposition of Rogue waves

We consider two distinct rogue wave solutions for u_1 and u_2 , and insert them in Eq. (4). We plot the resulting intensities $|\psi_1|^2$ and $|\psi_2|^2$ in Fig. 7. In the ψ_1 component the rogue waves merge together along with a periodic oscillation of the background. In the ψ_2 component we get a non-trivial twin peak rogue wave. Here too the background shows significant oscillations. To facilitate the understanding of the oscillations we explicitly present the expressions for $|\psi_1|^2$ and $|\psi_2|^2$. $|\psi_1|^2 = \frac{1}{4} \left(|\lambda_1|^2 + |\lambda_2|^2 + 2A \cos[2(|\delta^{(1)}|^2 - |\delta^{(2)}|^2)t] - 2B \sin[2(|\delta^{(1)}|^2 - |\delta^{(2)}|^2)t] \right)$ and

$$|\psi_2|^2 = \frac{1}{4} \left(|\lambda_1|^2 + |\lambda_2|^2 - 2A \cos[2(|\delta^{(1)}|^2 - |\delta^{(2)}|^2)t] + 2B \sin[2(|\delta^{(1)}|^2 - |\delta^{(2)}|^2)t] \right), \text{ where } \lambda_1 = \delta^{(1)} \left[1 - \frac{2(1+4i|\delta^{(1)}|^2 t)}{2|\delta^{(1)}|^2(x^2+4|\delta^{(1)}|^2 t^2 + \frac{1}{4|\delta^{(1)}|^2})} \right],$$

$$\lambda_2 = \delta^{(2)} \left[1 - \frac{2(1+4i|\delta^{(2)}|^2 t)}{2|\delta^{(2)}|^2(x^2+4|\delta^{(2)}|^2 t^2 + \frac{1}{4|\delta^{(2)}|^2})} \right], A \text{ and } B \text{ are real and imaginary parts of } \lambda_1 \lambda_2^*. \text{ From this expression we find that the oscillations originate from the circular functions (cosine and sine) appearing in the cross terms and depend upon}$$

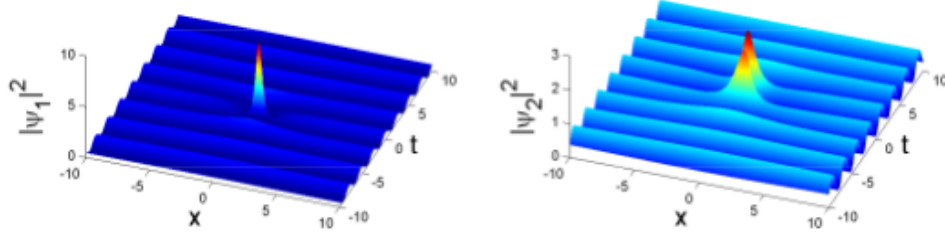


Figure 7: Superposition of two different rogue waves. The parameters are $\delta^{(1)} = \sqrt{1.5}$ and $\delta^{(2)} = \sqrt{0.3} - 0.1i$.

the difference $|\delta^{(1)}|^2 - |\delta^{(2)}|^2$. Especially, for $\delta^{(1)} = \delta^{(2)}$, the background oscillations are completely suppressed and the rogue wave appears only in the ψ_1 component while it disappears in the ψ_2 component.

Case (viii) Superposition of Rogue wave (u_1) with Akhmediev breather (u_2)

We choose the solution u_1 to admit rogue wave and u_2 to possess the form of Akhmediev breather. This type of superposition allows the possibility of interesting distinct nonlinear coherent structures in the ψ_1 and ψ_2 components. In the ψ_1 component the dominant behaviour is displayed by the rogue wave whose amplitude is increased significantly while that of the AB gets suppressed. The reverse scenario takes place in the ψ_2 component, that is, here the amplitude of the rogue wave is suppressed whereas that of the AB is enhanced significantly. This shows that there is an energy redistribution among the components. In both the components the background executes oscillations. Particularly in the ψ_2 component the background oscillates vibrantly. Such coherent structures are shown in Fig. 8.

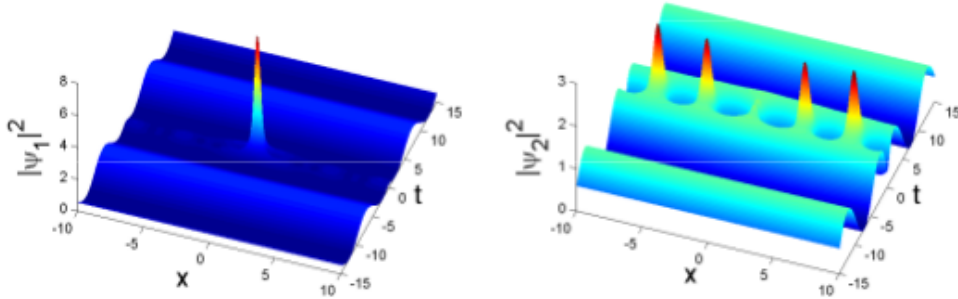


Figure 8: Superposition of rogue wave with Akhmediev breather for $\delta^{(1)} = \sqrt{1.5}$ and $a^{(2)} = 0.9$.

Case (ix) Superposition of Rogue wave (u_1) with Ma breather (u_2)

Finally, we consider the rogue wave solution for u_1 and Ma breather solution for u_2 in Eq. (4). The resulting intensity plots for the ψ_1 and ψ_2 components are shown in Fig. 9. This type of superposition results in nonlinear coherent structures with special dynamical properties. In the ψ_1 component the rogue wave appears predominantly. But it disappears completely in the ψ_2 component. In both the components the MB periodically reaches maximum and minimum intensities. Especially in the ψ_2 component the breather is dominant. Thus here too an energy redistribution takes place among the components ψ_1 and ψ_2 . Also, the background displays periodic oscillations in both the components.

In the following table, we have summarized all the above interesting nonlinear superposed coherent structures.

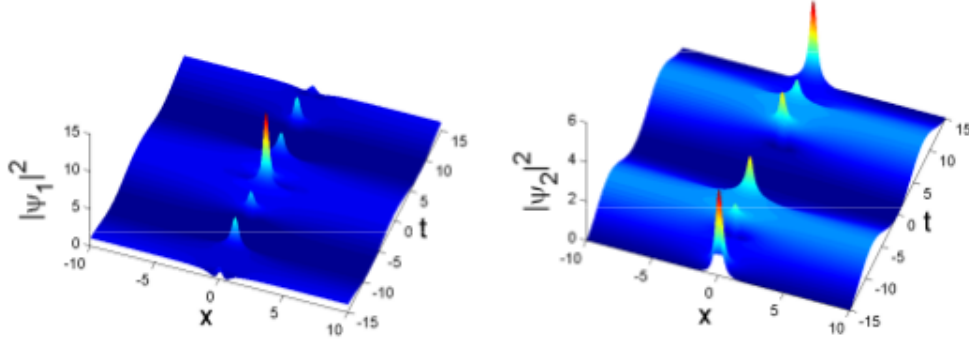


Figure 9: Superposition of rogue wave with Ma breather. The parameters are $\delta^{(1)} = \sqrt{1.2}$ and $a^{(2)} = 0.3$

Table 1: Superposition of several kinds of nonlinear waves

Case	Form of u_1	Form of u_2	Nature of nonlinear coherent structures	
			ψ_1 component	ψ_2 component
(i)	One-soliton	One-soliton	(a) Two soliton collision with higher intensity, (b) Oscillating bound soliton with larger period.	(a) Two soliton collision with lower intensity, (b) Oscillating bright soliton with smaller period.
(ii)	One-soliton	Two-soliton	(a) Collision of bound soliton with one soliton, (b) Three soliton collision with higher amplitude, and (c) Three soliton bound state.	(a) Similar behavior as in ψ_1 component, (b) Three soliton collision with lower amplitude, and (c) Three soliton bound state.
(iii)	One-soliton	Rogue wave	Coexistence of Ma breather with rogue wave.	
(iv)	One-soliton	Akhmediev breather	Coexistence of Ma and Akhmediev breathers with lower amplitude.	Coexistence of Ma and Akhmediev breathers with higher amplitude.
(v)	One-soliton	Ma breather	Colliding Ma breathers	
(vi)	Two-soliton	Rogue wave	(a) Coexistence of colliding Ma breathers with rogue wave (b) Bound state of Ma breathers with rogue wave	
(vii)	Rogue wave	Rogue wave	Higher amplitude rogue wave with oscillating background.	Lower amplitude twin peak rogue waves with oscillating background.
(viii)	Rogue wave	Ma breather	Rogue wave is dominant and Ma breather periodically reaches minimum and maximum intensities.	Ma breather is dominant.
(ix)	Rogue wave	Akhmediev breather	Rogue wave is dominant with higher amplitude and Akhmediev breather gets suppressed.	Akhmediev breather is dominant and rogue wave gets suppressed.

Apart from this we can have other possible superpositions such as (i) Two-soliton with Akhmediev breather, (ii) Two-soliton with Ma breather, (iii) Two-soliton with Two-soliton, (iv) Ma breather with Ma breather and (v) Akhmediev breather with Akhmediev breather. For brevity we don't discuss these cases here and the interested readers can explore these possibilities in a straightforward way.

4. Non-autonomous CCGP system

Next we turn our focus to the following non-autonomous CCGP system:

$$i\frac{\partial\psi_1}{\partial t} = \left[-\frac{\partial^2}{\partial x^2} + U_1(x, t) \right] \psi_1 - \alpha_1(t)(|\psi_1|^2 + 2|\psi_2|^2)\psi_1 - \alpha_2(t)\psi_2^2\psi_1^*, \quad (10a)$$

$$i\frac{\partial\psi_2}{\partial t} = \left[-\frac{\partial^2}{\partial x^2} + U_2(x, t) \right] \psi_2 - \alpha_1(t)(2|\psi_1|^2 + |\psi_2|^2)\psi_2 - \alpha_2(t)\psi_1^2\psi_2^*, \quad (10b)$$

with time-dependent nonlinearity coefficient $\alpha_j(t)$ and external potential $U(x, t)$. Here the external potentials $U_1 = U_2 = U(x, t) = \frac{1}{2}\Omega^2(t)x^2$.

4.1. Similarity transformation

First, we look for a similarity transformation that transforms the above non-autonomous CCGP system (10) into an integrable autonomous CCGP system. This will be of use in identifying the explicit forms of the variable nonlinearity coefficient and the nature of corresponding trapping potential which can support different nonlinear coherent structures in atomic systems.

For this purpose we introduce the following transformation for the dependent and independent variables in Eqs. (10) with $\alpha_1(t)=\alpha_2(t)=\alpha(t)$:

$$\psi_j(x, t) = \xi_1 \sqrt{2\alpha(t)} q_j(X(x, t), T(t)) e^{i\varphi(x, t)}, \quad j = 1, 2, \quad (11a)$$

where

$$\varphi(x, t) = \left[-\frac{1}{4} \frac{d}{dt} (\ln \alpha) \right] x^2 + \xi_1^2 \xi_2 \left(\alpha x - \xi_2 \xi_1^2 \int \alpha^2 dt \right) \quad (11b)$$

and the new coordinates X and T are defined as

$$X = \xi_1 \left(\alpha x - 2\xi_2 \xi_1^2 \int \alpha^2 dt \right), \quad T = \xi_1^2 \int \alpha^2 dt. \quad (11c)$$

Here ξ_j , $j = 1, 2$, are real arbitrary constants. Then Eq.(10) reduces to the following set of integrable equations [38]:

$$iq_{1,T} + q_{1,XX} + 2(|q_1|^2 + 2|q_2|^2)q_1 + 2q_2^2 q_1^* = 0, \quad (12a)$$

$$iq_{2,T} + q_{2,XX} + 2(|q_2|^2 + 2|q_1|^2)q_2 + 2q_1^2 q_2^* = 0, \quad (12b)$$

along with a constraint condition

$$\Omega^2(t) = \frac{2\dot{\alpha}^2 - \ddot{\alpha}\alpha}{2\alpha^2}, \quad (12c)$$

where the overdot denotes differentiation with respect to time t . Such type of transformation is possible mainly due to the temporal dependence of the nonlinearity and that of external harmonic potential; in the absence of such dependence these transformations are not at all possible. Now we can examine the dynamics of different nonlinear waves for a given type of nonlinearity and potential by expressing Eqs. (12) as two decoupled NLS equations using the transformation (4) and then by reconstructing ψ in terms of the original co-ordinates x and t by making use of the similarity transformation (11).

4.2. Forms of time- dependent nonlinear coefficient

Here we choose two types of nonlinearities namely, periodically and kink-like modulated nonlinearities, which are of physical interest in BECs.

(a) Periodically modulated nonlinearity

First we choose a periodic form for the nonlinearity coefficient, namely,

$$\alpha(t) = 1 + \epsilon \cos(t), \quad (13a)$$

where ϵ is a real arbitrary parameter. Such interesting periodic variations of the nonlinearity coefficient is considered in BECs [48]. This interesting nonlinearity is plotted in Fig. (10). The corresponding expression for $\Omega^2(t)$ is given by:

$$\Omega^2(t) = \frac{\epsilon[\cos(t) + \epsilon \cos^2(t) + 2\epsilon \sin^2(t)]}{2(1 + \epsilon \cos(t))^2}. \quad (13b)$$

(b) Kink-like nonlinearity

We also choose another form for variable nonlinearity co-efficient, given by

$$\alpha(t) = 2 + \tanh(\epsilon t), \quad (14a)$$

where ϵ is an arbitrary real function. In this case, we envision a nonlinearity that is rapidly varied from one value to another. The evolution of this nonlinearity is shown in Fig. (10). Such variation of nonlinearity has been observed in atomic BECs [49]. The corresponding form of $\Omega^2(t)$ is obtained as

$$\Omega^2(t) = \frac{\epsilon^2 \operatorname{sech}^2(\epsilon t)[1 + 2 \tanh(\epsilon t)]}{(2 + \tanh(\epsilon t))^2}. \quad (14b)$$

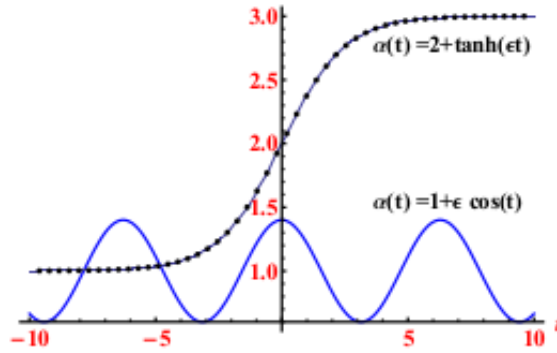


Figure 10: Typical form of periodically modulated and kink-like nonlinearity $\alpha(t)$ for $\epsilon = 0.4$.

4.3. Dynamics of superposed nonlinear waves in non-autonomous CCGP system

For brevity, here we consider three types of superposed non-autonomous nonlinear waves namely, superposition of two different non-autonomous solitons, superposition of two-soliton with a non-autonomous rogue wave and superposition of two different non-autonomous rogue waves. The general solution of the non-autonomous CCGP equations (10) can be constructed by using the transformations (11) and (4). It can be written as

$$\psi_1(x, t) = \xi_1 \sqrt{2\alpha(t)} e^{i\varphi(x,t)} (u_1(X, T) + u_2(X, T))/2, \quad (15a)$$

$$\psi_2(x, t) = \xi_1 \sqrt{2\alpha(t)} e^{i\varphi(x,t)} (u_1(X, T) - u_2(X, T))/2, \quad (15b)$$

where $u_1(X, T)$ and $u_2(X, T)$ can be any of the five solutions of NLS system (3) discussed in Sec. III A, with the

replacement of the old-coordinates x and t by the new co-ordinates X and T .

Case(i) Superposition of two different non-autonomous one solitons

Here, we have chosen u_1 and u_2 to be of the form given by Eq. (5) with x and t replaced by X and T , respectively. The periodically modulated nonlinearity affects both soliton velocity and its shape. This kind of oscillatory nonlinearity induces oscillations in the soliton profile and results in snake like propagation. Such non-autonomous solitons can be viewed as “creeping solitons”. This is shown in the top panel of Fig. 11.

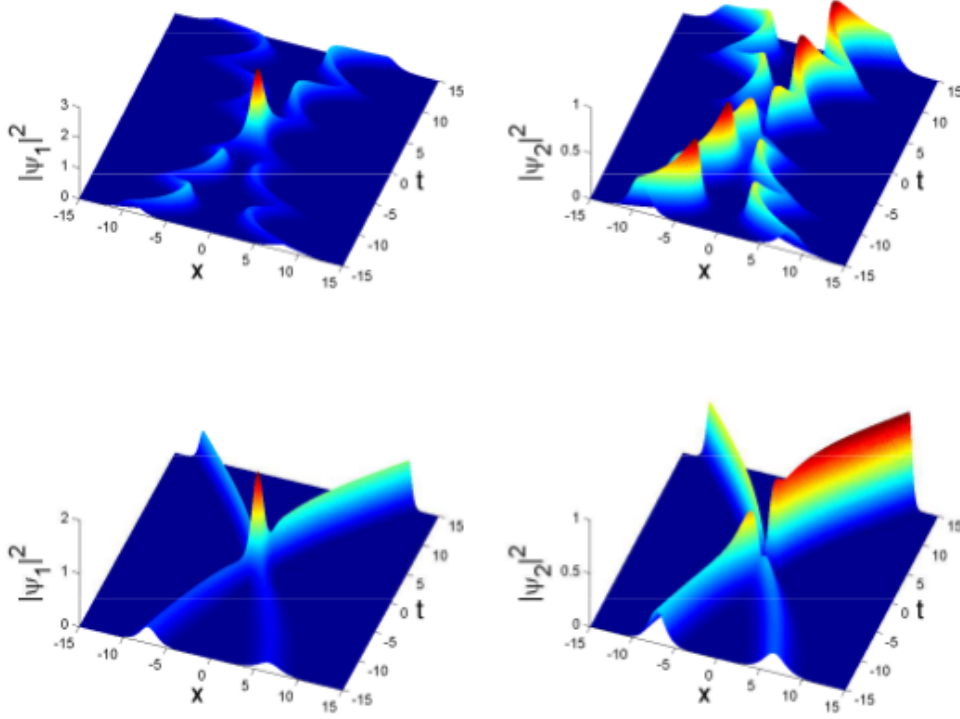


Figure 11: Superposition of two different one solitons. Top panel: Periodically modulated nonlinearity for $\epsilon = 0.4$, $\xi_1 = 0.8$ and $\xi_2 = 0$; Bottom panel: Kink-like nonlinearity for $\epsilon = 0.2$, $\xi_1 = 0.6$ and $\xi_2 = 0$. All other parameters are same as given in the top panel of Fig. 1.

Next, after introducing the kink nonlinearity, the direction of propagation is also affected (see Eq. (14a)), the shape and amplitude of the soliton are altered significantly by the inhomogeneity. Another interesting mechanism due to kink-like nonlinearity is “soliton compression”. This type of superposition looks similar to the collision of two one solitons. Here the amplitudes of the two solitons before collision are lower than that of after collision. After collision the width of the solitons (for large positive t) get compressed and their amplitudes are enhanced. Also the separation distance between two solitons before and after collision is different. In addition to this there is a bending in the path of the solitons during propagation due to the nature of nonlinearity. Such a dynamical behaviour is shown in the bottom panel of Fig. 11.

Case(ii) Superposition of two-soliton with rogue wave

In this case, we examine the superposition of two-soliton of the form (6a) with a rogue wave (7) in the presence of periodically modulated nonlinearity. Here, interestingly, the two-solitons are converted into breathers and the rogue wave remains as it is. A distinct feature of this nonlinearity is the wings of the breathers are stretched due to oscillation. Note that, here the background is oscillating in both the components in a periodic manner as compared with Fig. 6, where the periodically modulated nonlinearity is absent. This is shown in the top panel of Fig. 13 for illustrative purpose.

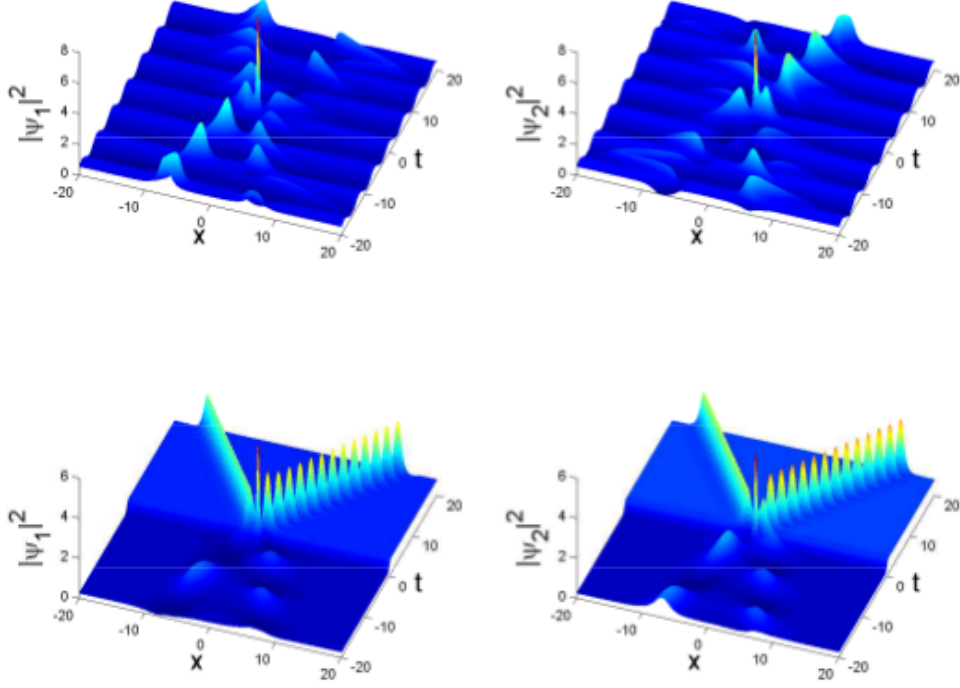


Figure 12: Superposition of two-solitons with a rogue wave. Top panel: Periodically modulated nonlinearity with parameters $\epsilon = 0.5$, $\xi_1 = 0.8$ and $\xi_2 = 0$. Bottom panel: Kink-like nonlinearity with parameters $\epsilon = 2.5$, $\xi_1 = 0.6$ and $\xi_2 = 0$. All other parameters are same as given in Fig. 6.

Next we consider the superposition of two non-autonomous solitons with a non-autonomous rogue wave in the presence of kink-like nonlinearity (see Eq. (14a)). This shows several dynamical features. First of all the background does not oscillate instead it displays a step-like profile. Here too the two-solitons are converted into breathers. Before collision the time period of breathers is greater whereas after collision it decreases and as a result of this the period of the breathers is narrowed down. Hence the number of breathers has enhanced after collision ($t > 0$). This is shown in the bottom panel of Fig. 13.

Case(iii) Superposition of non-autonomous rogue waves

By considering two different rogue waves in the presence of periodically modulated nonlinearity as given by Eq. (13a), we find that the period of oscillation in the background is well diminished as compared to that of Fig. 7 (autonomous case). In the second component we observe a non-trivial asymmetric twin peak rogue wave.

Next we consider the kink-like nonlinearity (see Eq. (14a)). Here the period of oscillating background is greater (almost suppressed) from $-\infty$ to 0 (see Fig. 7). For $t > 0$, the period of oscillation of background is decreased significantly with step-like enhancement in its background. This is shown in the bottom panel of Fig. 13. Also the intensity of the rogue wave is increased significantly in the ψ_1 and ψ_2 components as compared with that of Fig. 7.

5. Conclusions

In conclusion, we have studied the superposed nonlinear waves of coherently coupled GP system. Based on a set of linear transformations, the coherently coupled GP equations are converted into two decoupled NLS equations. We briefly discuss the available nonlinear wave solutions of scalar NLS equation, namely solitons (one- and two-), rogue waves and breathers (Ma- and Akhmediev). We show that the existence of various interesting coherent nonlinear structures such as, collision of bound soliton with soliton, three soliton collision, coexistence of rogue wave and Ma

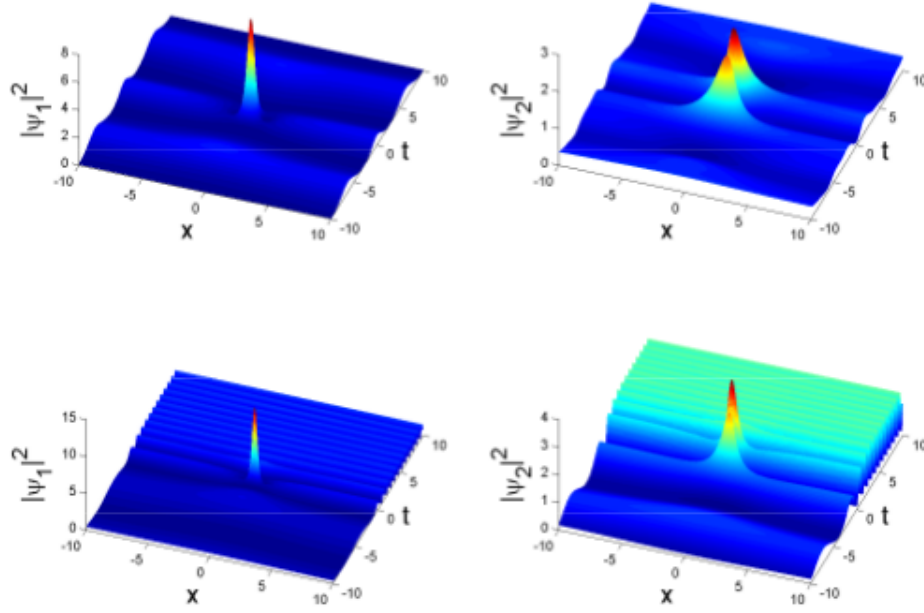


Figure 13: Superposition of rogue wave with another rogue wave. Top panel: Periodically modulated nonlinearity with parameters $\epsilon = 0.4$, $\xi_1 = 0.6$ and $\xi_2 = 0.1$. Bottom panel: Kink-like nonlinearity with parameters $\epsilon = 0.5$, $\xi_1 = 0.6$ and $\xi_2 = 0$. All other parameters are same as given in Fig. 7.

breather, coexistence of Ma and Akhmediev breathers, collision of Ma breathers, bound state of Ma breather by superimposing different types of nonlinear waves. We have also shown that by such superposition the conventional rogue waves and breathers (Ma/Akhmediev) can be engineered. Finally, we consider the non-autonomous CCGP system with physically relevant time-dependent nonlinearity coefficients and external potential. With the aid of a similarity transformation, the non-autonomous CCGP system is converted into an integrable autonomous CCGP system with a constraint condition. We examine the two forms of nonlinearity coefficient, namely kink-like and periodically modulated function and investigate their effects on the novel coherent structures of superposed nonlinear waves. Especially, we demonstrate the possibility of manipulating the nonlinear waves in autonomous as well as non-autonomous settings of the CCGP systems.

Acknowledgments. The work of T.K. is supported by Department of Science and Technology, Government of India, in the form of a major research project. The authors acknowledge the Principal and Management of Bishop Heber College (Autonomous), Tiruchirappalli for the constant support and encouragement. The authors also thank K. Sakkaravarthi for useful discussions.

References

References

- [1] A.C. Scott, *Nonlinear Science: Emergence and Dynamics of Coherent Structures* (Oxford University Press, Oxford, 1999)
- [2] M.J. Ablowitz and H. Segur, *Solitons and the Inverse Scattering Transform* (SIAM, Philadelphia, 1981).
- [3] G.B. Whitham, *Linear and Nonlinear Waves* (Wiley, New York, 1974).
- [4] P.G. Kevrekidis, D.J. Frantzeskakis and R. Carretero-González (Eds.) *Emergent Nonlinear Phenomena in Bose-Einstein Condensates: Theory and Experiment* (Springer, 2008).
- [5] P.A. Ruprecht, M.J. Holland and K. Burnett, Phys. Rev. A **51** 4704 (1995); D.J. Frantzeskakis, J. Phys. A: Math. Theor. **43** (2010) 213001.
- [6] R. Campbell, G.L. Oppo and M. Borkowski, Phys. Rev. E **91** (2015) 012909.
- [7] Yu.V. Bludov, V.V. Konotop and N. Akhmediev, Phys. Rev. A **80** (2009) 033610; Yu.V. Bludov, Z.Y. Yan and V.V. Konotop, Phys. Rev. A **81** (2010) 063610; L. Wen, L. Li, Z.D. Li, S.W. Song, X.F. Zhang and W.M. Liu, Euro. Phys. J.D **64**, 473 (2011).

- [8] P. Engels, C. Atherton and M.A. Hoefer, Phys. Rev. Lett. **98** (2007) 095301.
- [9] B.J. Dabrowska-Wüster, E.A. Ostrovskaya, T.J. Alexander and Y.S. Kivshar, Phys. Rev. A **75** (2007) 023617.
- [10] J.E. Williams and M.J. Holland, Nature (London) **401** (1999) 568; A.A. Svidzinsky and A.L. Fetter, Phys. Rev. A **62** (2000) 063617.
- [11] A. Smerzi, S. Fantoni, S. Giovanazzi and S.R. Shenoy, Phys. Rev. Lett. **79** (1997) 4950; T. Zibold, E. Nicklas, C. Gross and M.K. Oberthaler, Phys. Rev. Lett. **105** (2010) 204101.
- [12] J.P. D'Incao and B.D. Esry, Phys. Rev. A **73** (2006) 030703(R).
- [13] K. Kasamatsu, M. Tsubota and M. Ueda, Phys. Rev. A **71** (2005) 043611.
- [14] Y.-J. Lin, K. Jiménez-García and I.B. Spielman, Nature (London) **471** (2011) 83.
- [15] C.J. Myatt, E. A. Burt, R.W. Ghrist, E.A. Cornell and C.E. Wieman, Phys. Rev. Lett. **78** (1997) 586; D.S. Hall, M.R. Matthews, J.R. Ensher, C.E. Wieman and E.A. Cornell, Phys. Rev. Lett. **81** (1998) 1539.
- [16] A. Sartori, J. Marino, S. Stringari and A. Recati, New J. Phys. **17** (2015) 093036.
- [17] M. Tylutki, L.P. Pitaevskii, A. Recati and S. Stringari, Phys. Rev. A **93** (2016) 043623.
- [18] M. Abad and A. Recati, Eur. Phys. J. D **67** (2013) 148.
- [19] L.C. Zhao, L. Ling, Z.Y. Yang and J. Liu, Commun. Nonlinear Sci. Numer. Simulat. **23** (2015) 3.
- [20] C. Menotti, F. Minganti and A. Recati, Phys. Rev. A **93** (2016) 033602.
- [21] Ph. Courteille, R.S. Freeland, D.J. Heinzen, F.A. van Abeelen and B.J. Verhaar, Phys. Rev. Lett. **81**, 69 (1998); S. Inouye, M.R. Andrews, J. Stenger, H.-J. Miesner, D.M. Stamper-Kurn and W. Ketterle, Nature (London) **392** (1998) 151; I. Bloch, J. Dalibard and W. Zwerger, Rev. Mod. Phys. **80** (2008) 885.
- [22] C.A. Regal, M. Greiner and D.S. Jin, Phys. Rev. Lett. **92** (2004) 040403; M. Greiner, C.A. Regal and D.S. Jin, Phys. Rev. Lett. **94** (2005) 070403.
- [23] W.P. Zhong, M. Belić and B.A. Malomed, Phys. Rev. E **92** (2015) 053201; J. Belmonte-Beitia, V.M. Pérez-García V. Vekslerchik, and V.V. Konotop Phys. Rev. Lett. **100** (2008) 164102; Y.V. Kartashov, B.A. Malomed and L. Torner, Rev. Mod. Phys. **83** (2011) 247; J.S. He, E.G. Charalampidis, P.G. Kevrekidis and D.J. Frantzeskakis, Phys. Lett. A **378** (2014) 577; C.G.L. Tiofack, S. Coulibaly and M. Taki, Phys. Rev. A **92** (2015) 043837.
- [24] F. Tsitoura, P. Krüger, P.G. Kevrekidis and D.J. Frantzeskakis, Phys. Rev. A **91** (2015) 033633; T. Kanna, R. Babu Mareeswaran, F. Tsitoura, H.E. Nistazakis and D.J. Frantzeskakis, J. Phys. A: Math. Theor. **46** (2013) 475201; R. Babu Mareeswaran, E.G. Charalampidis, T. Kanna, P.G. Kevrekidis and D.J. Frantzeskakis, Phys. Rev. E **90** (2014) 042912.
- [25] F.K. Abdullaev, A.M. Kamchatnov, V.V. Konotop and V.A. Brazhnyi, Phys. Rev. Lett. **90** (2003) 230402; F.K. Abdullaev, A. Gammal and L. Tomio, J. Phys. B: At. Mol. and Opt. Phys. **49** (2015) 025302.
- [26] H. Saito, R.G. Hulet and M. Ueda, Phys. Rev. A **76** 053619 (2007); J. Williams, R. Walser, J. Cooper, E.A. Cornell and M. Holland, Phys. Rev. A **61** (2000) 033612.
- [27] P.J. Everitt, M.A. Sooriyabandara, G.D. McDonald, K.S. Hardman and C. Quinlivan, arXiv: 1509.06844v1 (2015).
- [28] D.R. Solli, C. Ropers, P. Koonath and B. Jalali, Nature (London) **450** (2007) 1054.
- [29] T.B. Benjamin and J.E. Feir, J. Fluid Mech. **27** (1967) 417.
- [30] D.H. Peregrine, J. Aust. Math. Soc. Ser. B **25** (1983) 16.
- [31] Yu.V. Bludov, V.V. Konotop and N. Akhmediev, Eur. Phys. J. Special Topics **185** (2010) 169; Yu.V. Bludov, V.V. Konotop and N. Akhmediev, Phys. Rev. A **80** (2009) 033610.
- [32] Z.Y. Qin and G. Mu, Phys. Rev. E **86** (2012) 036601.
- [33] F. Baronio, A. Degasperis, M. Conforti and S. Wabnitz, Phys. Rev. Lett. **109** (2012) 044102 ; F. Baronio, M. Conforti, A. Degasperis, S. Lombardo, M. Onorato and S. Wabnitz, Phys. Rev. Lett. **113** (2014) 034101.
- [34] M. Onorato, S. Residori, U. Bortolozzo, A. Montina and F.T. Arecchi, Phys. Rep. **528** (2013) 47; P.T.S. DeVore, D.R. Solli, D. Borlaug, C. Ropers and B. Jalali, J. Opt. **15** (2013) 064001.
- [35] N. Akhmediev and V.I. Korneev, Theor. Math. Phys. **69** (1986) 1089.
- [36] Y.C. Ma, Stud. Appl. Math. **60** (1979) 43.
- [37] Q.H. Park and H.J. Shin, Phys. Rev. E **59** (1999) 2373.
- [38] T. Kanna, M. Vijayayanthi and M. Lakshmanan, J. Phys. A: Math. Theor. **43** (2010) 434018; T. Kanna and K. Sakkaravarthi, J. Phys. A: Math. Theor. **44** (2011) 285211.
- [39] L.C. Zhao, L. Ling, Z.Y. Yang and J. Liu, Commun. Nonlinear Sci. Numer. Simulat. **23** (2015) 21.
- [40] H.E. Nistazakis, D.J. Frantzeskakis, P.G. Kevrekidis, B.A. Malomed, and R. Carretero-Gonzalez, Phys. Rev. A **77** (2008) 033612.
- [41] Y.S. Kivshar and G.P. Agrawal, *Optical Solitons: From Fibers to Photonic Crystals* (San Diego: Academic, 2003).
- [42] R.L. Horne, P.G. Kevrekidis, and N. Whitaker, Phys. Rev. E **73** (2006) 066601.
- [43] A. Chabchoub, N.P. Hoffmann and N. Akhmediev, Phys. Rev. Lett. **106** 204502 (2011); A. Chabchoub and M. Fink, Phys. Rev. Lett. **112** (2014) 124101.
- [44] T. Kanna and M. Lakshmanan, Phys. Rev. Lett. **86** 5043 (2001); T. Kanna and M. Lakshmanan, Phys. Rev. E **67** (2003) 046617.
- [45] B. Kibler, J. Fatome, C. Finot, G. Millot, F. Dias, G. Genty, N. Akhmediev and J.M. Dudley, Nature Physics **6** (2010) 790; J.M. Dudley, F. Dias, M. Erkintalo and G. Genty, Nature Photonics **8** (2014) 755.
- [46] M. Lakshmanan and S. Rajasekar, *Nonlinear dynamics: Integrability, chaos and patterns* (Springer-Verlag, Berlin, 2003).
- [47] A. Chabchoub, N. Hoffmann, M. Onorato and N. Akhmediev, Phys. Rev. X **2** (2012) 011015.
- [48] H. Saito and M. Ueda, Phys. Rev. Lett. **90** (2003) 040403; P.G. Kevrekidis, G. Theocharis, D.J. Frantzeskakis and B.A. Malomed, Phys. Rev. Lett. **90**, 230401 (2003); F.Kh. Abdullaev, A.M. Kamchatnov, V.V. Konotop and V.A. Brazhnyi, Phys. Rev. Lett. **90** (2003) 230402; F.Kh. Abdullaev, J.G. Caputo, R.A. Kraenkel and B.A. Malomed, Phys. Rev. A **67** (2003) 013605.
- [49] S.E. Pollack, D. Dries, M. Junker, Y.P. Chen, T.A. Corcovilos and R.G. Hulet, Phys. Rev. Lett. **102** (2009) 090402.